Numerical and Experimental Evaluation of Solar Air Heaters Connected in Series

R. Pérez-Espinosa, O. García-Valladares, I. Pilatowsky

Instituto de Energías Renovables, Universidad Nacional Autónoma de México, Privada Xochicalco S/N, Centro, CP 62580, Temixco, Morelos, México, jrpee@ier.unam.mx, ogv@ier.unam.mx, ipf@ier.unam.mx

Abstract

A numerical and experimental evaluation of three solar air heaters (SAHs) arrangement was carried out. The numerical model uses the control volume finite element method with discretization in longitudinal and axial direction using empirical correlations to solve the energy equation in a short time; as a result, the numerical model calculates the coefficients of linear and quadratic instantaneous thermal efficiency curves, the incident angle modifier, and the temperature and humidity profile in the air flow and the temperature profiles in solid materials. The experimental tests were carried out according to the methods described on the international standard ISO9806:2017. A comparison of the thermal efficiency curves obtained for one, two and three SAHs connected in series operating at $0.087 m^3 s^{-1}$ was carried out. The thermal efficiency experimental data was used to validate the numerical model, resulting in a ±0.03 absolute error.

Keywords: solar energy; numerical model; thermal efficiency; solar collectors

1. Introduction

One of the main areas of action to reduce food losses and waste is the improvement of conservation technologies. However, solutions to minimize losses usually involve greater energy use, especially in the conservation of food products (Sharma et al., 2009). The need for sustainability, food security, and to decouple food prices from the fluctuating prices of finite fossil fuels have driven the search for sustainable processing and the adequate storage of agricultural products. The correct design and optimization of Solar Air Heaters (SAHs) used for drying food can be fundamental to achieve this purpose.

SAHs are used to get hot air for the drying of both agricultural and sea products and for heating buildings, principally in places with cold weather (Tchinda, 2009). In order to improve these devices, several researchers have designed different configurations around the world (Al-Kamil & Al-Ghareeb, 1995). With the development of computer, hardware and numerical methodology, advanced mathematical models are being used to carry out important investigations on SAH (Tchinda, 2009). The aim of this work is carried out the numerical and experimental evaluation of thermal performance on one, two and three SAHs connected in series.

2. Theoretical fundamentals

2.1 Axial and longitudinal discretization

In order to carry out a thermal analysis of SAHs, the domain was discretized in both axial

doi:10.18086/swc.2019.13.02 Available at http://proceedings.ises.org

and longitudinal directions (Pérez-Espinosa & García-Valladares, 2018). Figs. 1 and 2 show the nodes distribution used for the thermal analysis.

2.2 Energy balance equation

The following general equation was obtained with an energy balance in each control volume in order to determine the temperature in each analyzed node (Pérez-Espinosa & García-Valladares, 2019):

$$(C_N + C_S + C_E + C_W)T_{i,j} = C_N T_{i+1,j} + C_S T_{i-1,j} + C_E T_{i,j+1} + C_W T_{i,j-1} + q_{g,i,j} \qquad \text{(eq. 1)}$$

Where C is the thermal resistance between the neighbor nodes (the subscripts N, S, E and W are the north, south, east and west neighbor), T is the temperature in the (i,j) node and q_g is the term of heat generation in the (i,j) node.

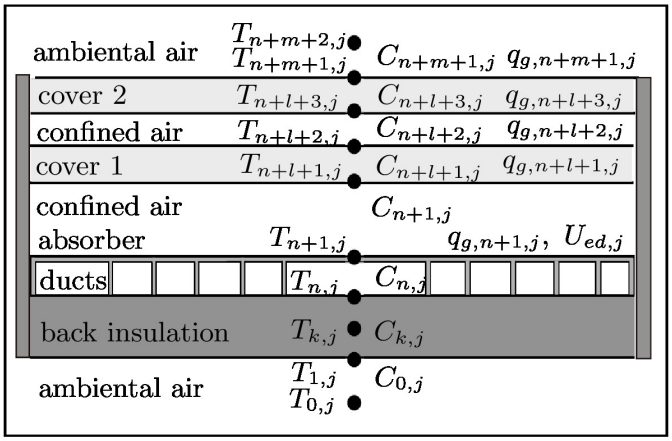

Fig. 1. Axial discretization of the SAH.

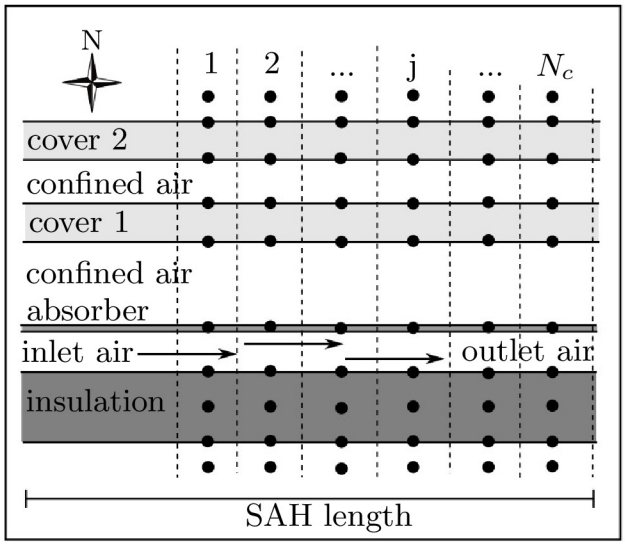

Fig. 2. Longitudinal discretization of the SAH.

2.3 Instantaneous thermal efficiency

The instantaneous thermal efficiency allows determine the portion of the heat transferred to the air flow and it is calculated according to eq. (2) (ISO 9806, 2017).

$$\eta = \frac{\dot{m}Cp(T_{out} - T_{\text{in}})}{GA} \qquad \text{(eq. 2)}$$

Where $\dot{m}$ is the mass flow rate, Cp is the air specific heat at constant pressure, T_{out} and T_{in} are the temperatures of the air at the outlet and at the inlet of the SAH respectively, G is the solar irradiance and A is the gross area of the SAH.

3. Experimental tests

3.1. Material and methods

The equipment and devices used to carry out the experimental test are listed as follow: three SAHs, one industrial fan, one volumetric flow meter, one pyranometer, nine PT1000 sensors, two humidity sensors and one RTD sensor. Fig. 3 shows experimental set up developed for the tests and Table 1 shows the uncertainty of the sensors used.

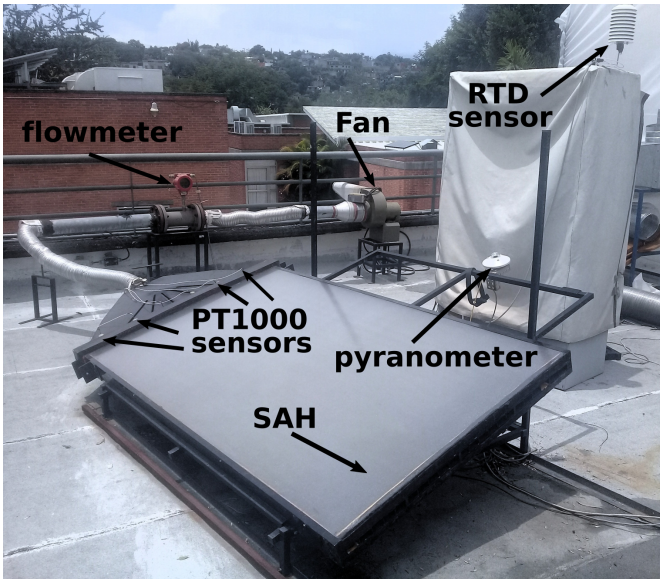

Fig. 3. The experimental set up with one SAH.

Table. 1. Parameters and associated uncertainty for measurement sensors.

Parameter	Instrument	Uncertainty
Solar irradiance	Pyranometer-class II	±11.54W m^{-2}
Volumetric flow rate	Velocity sensor	±1.76m^3 s^{-1}
Ambient temperature	Thermistor	±0.06°C
Inlet air temperature	Thermistor	±0.12°C
Outlet air temperature	Thermistor	±0.12°C
Air humidity	Microcontroller	±0.01 kgH_2O kg dry air^{-1}

Three arrangements were used in this work; these tests consisted in one, two and three SAHs connected in series with a volumetric air flow rate of 0.087m^3s^{-1}. All the procedure used to evaluate the thermal performance of SAHs was based on the international standard ISO 9806:2017 (ISO 9806, 2017).

4. Validation

Eq. (3) is used to determine the percentage of absolute error (Ea) obtained between the experimental instantaneous thermal efficiency values (η_{exp}) against the obtained by the numerical model (η_{num}),

$$Ea = (\eta_{exp} - \eta_{num}) \qquad \text{(eq. 3)}$$

Figs. 4, 5 and 6 show the comparison between the thermal efficiency curves obtained with both experimental data with their respective error bars and numerical results with a volumetric air flow rate of $0.087 m^3 s^{-1}$.

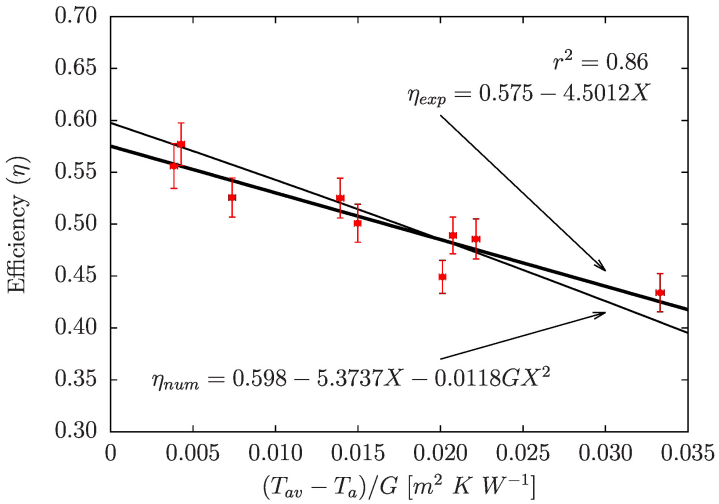

Fig. 4. Thermal efficiency curves for one SAH.

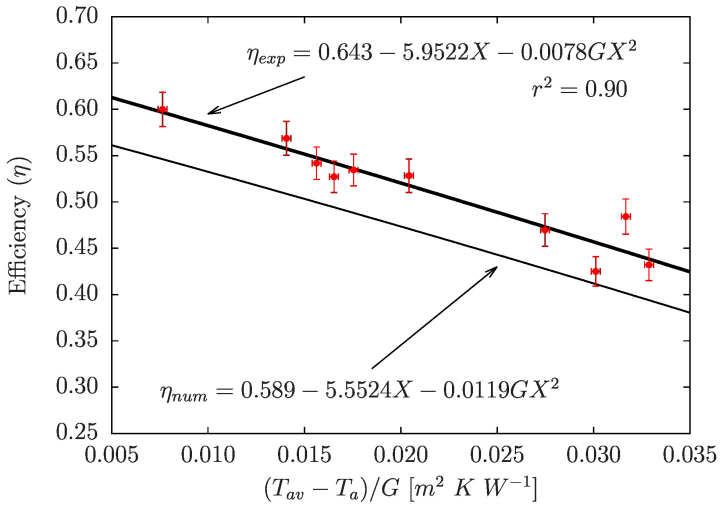

Fig. 5. Thermal efficiency curves for two SAHs connected in series.

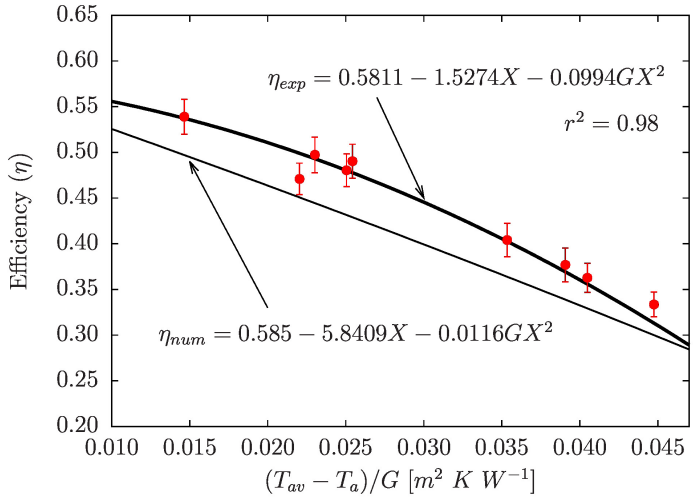

Fig. 6. Thermal efficiency curves for three SAHs connected in series.

Fig. 6 shows that the experimental data are above of the values obtained by the numerical simulation; this behavior also is showed in the comparison of the two SAHs arrangement in (see Fig. 5). Only in the one SAH arrangement (see Fig. 4), both the experimental and numerical thermal efficiency curves show similar values with low absolute errors. The differences obtained in Figs. 4 and 5 may be due to the interface between the SAHs. The discontinuity in the ducts increase the turbulence of the air flow and this phenomenon is not considered in the numerical model.

The absolute error obtained for the one, two and three SAHs arrangements were 0.01, -0.04 and -0.05 respectively, with an average error of ±0.03.

5. Results

Fig. 7 shows the comparison between the instantaneous thermal efficiency curves obtained for one, two and three SAHs connected in series operating with a volumetric air flow rate of 0.087m^3s^{-1}.

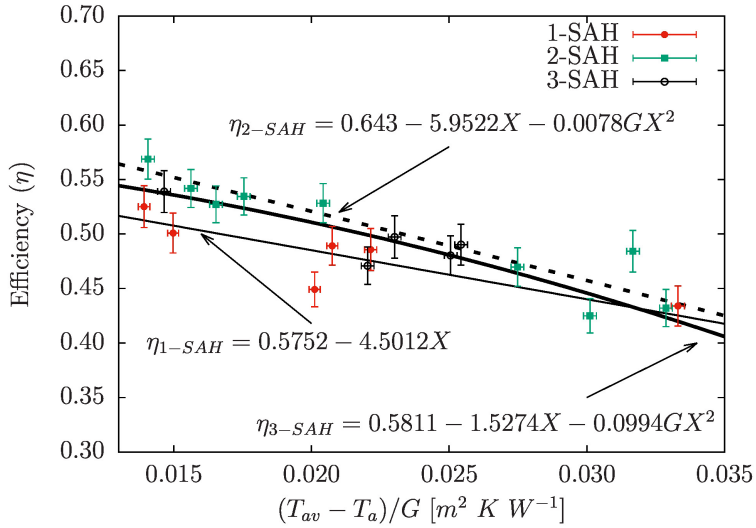

Fig. 7. Comparison between three SAHs connected in series with a volumetric flow rate of 0.087m^{3}s^{-1}.

Fig. 7 shows that the instantaneous thermal efficiency is significantly increased for the 2 SAHs arrangement compared with the 1-SAH arrangement, however, when the 3 SAHs arrangement is used the instantaneous thermal efficiency decrease compared with the 2 SAHs.

Although the instantaneous thermal efficiency for the 3 SAHs arrangement is not so different, Fig. 8 shows that the temperature reached for each arrangement is so different as it was expected. Experimentally, for a 30.34°C inlet temperature, the system with one, 2 and 3 SAHs arrangements reached an outlet temperature of 45.05°C, 63.98°C and 74.77°C respectively. Additionally, Fig. 8 shows the numerical temperature profiles for one, 2 and 3 SAHs arrangements, which reached an outlet temperature of 45.97°C, 58.40°C, and 71.36°C respectively. These results together with the instantaneous thermal efficiency curve are very useful for the design and development of solar drying or heating systems.

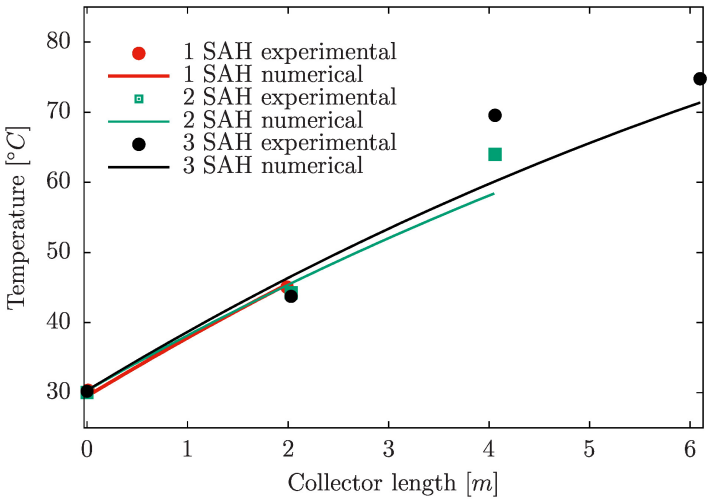

Fig. 8. Temperature profiles for one, 2 and 3 SAHs arrangements.

6. Concluding remarks

A numerical model to evaluate the thermal performance of rectangular ducts solar air heaters (SAHs) was successfully developed. This model determines the linear and quadratic instantaneous thermal efficiency curves, the incident angle modifier, and the temperature and humidity profiles in the air flow and the temperature profiles in solid materials. The numerical model was validated using the experimental efficiency data, obtaining a ±0.03 of absolute error. Once the numerical model was validated, a study of the dependence of the arrangements in the thermal efficiency of SAHs was carried out. The results show that the 2 SAHs configuration is a good arrangement because it is obtained a higher instantaneous thermal efficiency compared with the 1 SAH arrangement and, had it had almost the same instantaneous thermal efficiency of the 3 SAHs arrangement; however, if operation air temperatures between 64 – 75 °C are needed, only the 3 SAHs arrangement can supply these thermal conditions.

7. Acknowledgment

This work was partially supported by the following projects: FORDECYT Project No. 190603, CEMIE-Sol Project No. 12 and PRODETES award. A special acknowledgement to Módulo Solar SA de CV for the manufacture of the solar air heaters.

8. References

Al-Kamil, M. T., & Al-Ghareeb, A. A. (1997). Effect of thermal radiation inside solar air heaters. *Energy conversion and management*, *38*(14), 1451-1458.

ISO, E. (2017). 9806: 2017. *Solar energy–Solar thermal collectors–Test methods*.

Pérez-Espinosa, R., & García-Valladares, O. (2018). Solar Collector Simulator (SolCoSi): A new validated model for predicting the thermal performance of flat plate solar collectors. *Journal of Renewable and Sustainable Energy*, *10*(1), 013705.

Pérez-Espinosa, R., & García-Valladares, O. (2019). Numerical modeling and experimental validation of Back-Pass rectangular ducts solar air heaters. *Accepted in Applied Thermal Engineering*.

Sharma, A., Chen, C., Lan, N.V. (2009). Solar-energy drying systems: A review. *Renewable and Sustainable Energy Reviews*, 13, 1185-1210.

Tchinda, R. (2009). A review of the mathematical models for predicting solar air heaters systems. *Renewable and sustainable energy reviews*, *13*(8), 1734-1759.

Appendix: units and symbols

Tab. A1: Nomenclature.

Quantity		Unit	Quantity	Symbol	Unit
Absolute error	Ea	- -	Experimental	*exp*	
Area	A	m^{-2}	i-th node	*i*	
Thermal resistance	*C*	W m^{-2} K^{-1}	Inlet	in	
Specific heat at constant pressure	Cp	J kg^{-1} K^{-1}	j-th node	*j*	
Solar irradiance	G	W m^{-2}	k-th node	k	
Mass flow rate	$\dot{m}$	kg s^{-1}	l-th node	*l*	
Number of control volumes	N_c	- -	Number of nodes at the cover	*m*	
Heat flux	q_g	W m^{-2}	Number of nodes at the back insulation	n	

Temperature	T	K	Numerical	num
Heat transfer coefficient at the edges	U_{ed}	W m^{-2} K^{-1}	North	N
Thermal parameter	X	m^2 K W^{-1}	Outlet	out
			South	S
Subscripts			West	W
Ambiental	a			
Average	av		*Greek*	
East	E		Thermal efficiency	η